PIER AND ABUTMENT SCOUR: INTEGRATED APPROACH

By Bruce W. Melville[1]

ABSTRACT: This paper summarizes many of the results from an extensive program of bridge scour research undertaken at The University of Auckland, New Zealand. An integrated approach to the estimation of local scour depth at bridge piers and abutments, collectively termed bridge foundations, is presented. The design method is based on empirical relations, termed K-factors, that account for the effects on scour depth of flow depth and foundation size, flow intensity, sediment characteristics, foundation type, shape and alignment, and approach channel geometry. The K-factors are evaluated by fitting envelope curves to existing data for piers and abutments and a new extensive data set for abutments. The new data are discussed and presented. Application of the design method is illustrated in examples.

INTRODUCTION

An analogy between the mechanisms of local scouring at bridge piers and abutments, collectively called bridge foundations here, has long been recognized (Shen et al. 1966; Lemos 1975). The flow structure and associated scour process at an abutment are considered to be similar to that at a pier of shape equivalent to the abutment and its mirror image in the channel wall. The scour depth at the abutment is acknowledged to be less than that at the analogous pier due to the channel wall effects on retarding the flow.

Various studies of the flow structure at bridge foundations have been undertaken, including those by Melville (1975), Melville and Raudkivi (1977), Hjorth (1975), Parola et al. (1994), Kwan (1988), and Kwan and Melville (1994). These studies generally confirm the similarity of the flow in and around the scour hole at piers and abutments, particularly where the abutment extends only a short distance into the channel in relation to the depth of flow, i.e., at a relatively short abutment. Thus, the dominant flow component at shorter abutments closely resembles one side of the horseshoe vortex and associated downflow, which are important in the development of scour at bridge piers. At piers, the deepest scour occurs on the line of symmetry, while the scour depth along the upstream face of shorter abutments is reasonably uniform and therefore similar to that at piers.

For longer abutments, Kwan (1984) identified the principal flow components as depicted in Fig. 1(a). He called the strong spiral flow, shown as the larger curled arrows in Fig. 1(a), the principal vortex because of its significance in the scour process and also noted the induced secondary (counterrotating) vortex around the edge of the scour hole and the sand ridge between the two vortices. Kwan (1984) and Kandasamy (1989) found that the area of quiescent fluid ahead of the abutment near the channel wall, shown in Fig. 1(a) as a weak counterrotating eddy, also influences the scour development, particularly at longer abutments. The outer limit of the area of quiescent fluid can be considered to demarcate the surface of an "effective" abutment, because the fluid within this area does not affect the scour process. The relative extent of this area of fluid increases with abutment length and, at longer abutments, the large area of quiescent fluid protects the sediment bed near the channel wall from erosion. The scour hole extends only part way along the upstream face of the abutment, as shown in Fig. 1(a).

In this paper, an integrated approach to the estimation of the depth of local scour at piers and abutments is presented. The paper summarizes many of the results from a comprehensive program of bridge scour research undertaken at The University of Auckland, New Zealand over a period of 25 years. The method presented is consistent with the design methods in Melville and Sutherland (1988) for piers and Melville (1992) for abutments. Data given in the earlier papers are augmented with more recent data, especially for abutment scour. Most of the new data were measured by Dongol (1994). These data both complement those presented in Melville (1992) for the effects of particular parameters and provide new data for parameters not previously studied, including sediment size and gradation and compound channel geometry. Dongol (1994) also made measurements of scour at abutments for bridges with very long approach embankments.

ESTIMATION OF LOCAL SCOUR DEPTH

Local scour is a time-dependent process. The temporal maximum scour depth (for a given set of conditions) is termed the equilibrium depth of scour. At equilibrium, the local scour depth at a bridge foundation can be described by

$$d_s = K_{yW} K_I K_d K_s K_\theta K_G \tag{1}$$

where K = empirical expressions accounting for the various influences on scour depth; K_{yW} = depth size $\equiv K_{yb}$ for piers and K_{yL} for abutments; K_I = flow intensity; K_d = sediment size; K_s = pier or abutment shape; K_θ = pier or abutment alignment; and K_G = channel geometry. Following the earlier papers, K_I is formulated to include sediment gradation effects as well as flow velocity effects. K_{yW} and d_s have the dimension of length, while the other Ks are dimensionless. Eq. (1) applies to local scour and is restricted to bridge crossings where the contraction effects, as represented by the ratio of the widths of the bridge opening and channel, are insignificant.

The various parameters are now considered individually. Envelope curves are drawn to the known valid laboratory data to define the K-factors.

Flow Depth-Foundation Size

Using a three-dimensional plot of laboratory data, Kandasamy (1989) identified various zones of dependence of d_s on flow depth (y) and the transverse dimension of the pier (b) or abutment (L), collectively symbolized by W. For deep flows compared to the pier or abutment size, Kandasamy concluded that the scour depth increases proportionately with W, but is independent of y. This finding was not new for piers, being consistent with many earlier studies, for example: Chabert and Engeldinger (1956), Ettema (1980), Raudkivi (1986), and Melville and Sutherland (1988). Ettema (1980) explained that for shallow flows, the surface roller that forms ahead of the bridge pier interferes with the scour action of the horseshoe vortex

[1]Sr. Lect., Dept. of Civ. and Resour. Engrg., The Univ. of Auckland, Auckland, New Zealand.

Note. Discussion open until July 1, 1997. To extend the closing date one month, a written request must be filed with the ASCE Manager of Journals. The manuscript for this paper was submitted for review and possible publication on June 9, 1995. This paper is part of the ***Journal of Hydraulic Engineering***, Vol. 123, No. 2, February, 1997. ©ASCE, ISSN 0733-9429/97/0002-0125–0136/$4.00 + $.50 per page. Paper No. 10923.

(a)

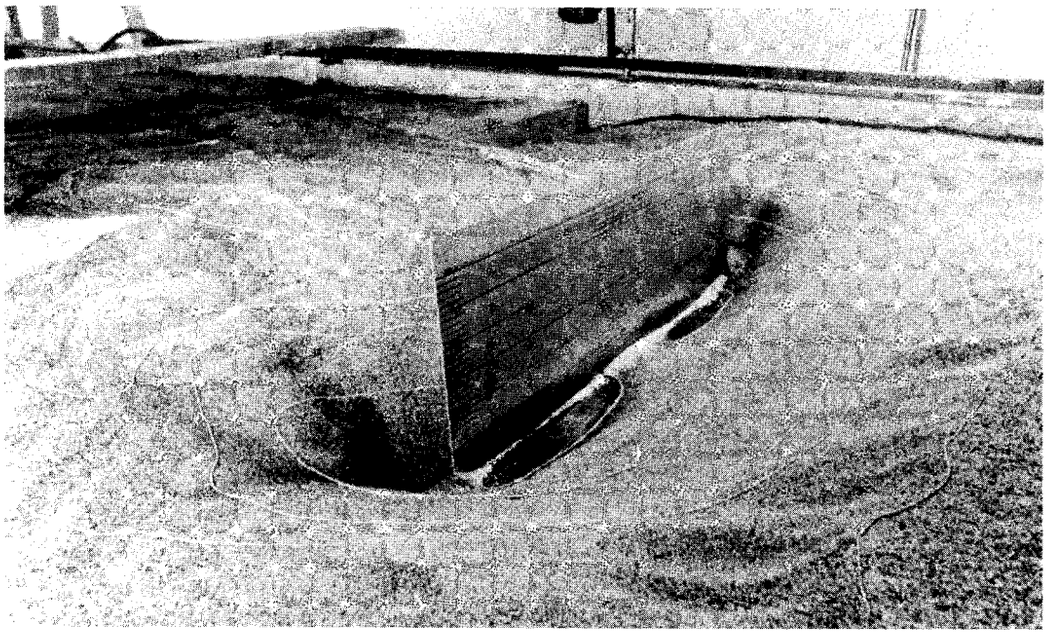

(b)

FIG. 1. (a) Pictorial Representation of Principal Flow Components at a Long Abutment [Kwan (1984)]; (b) Scour Hole at Very Wide Vertical-Wall Pier

because the two have opposite senses of rotation. With increasing flow depth, the interference reduces and eventually becomes insignificant. However, the conclusion represented a new concept for abutment scour. For shallow flows compared to the pier or abutment size, the scour depth increases proportionately with y, but is independent of W, while for intermediate depth flows, d_s depends on both y and W, according to Kandasamy (1989).

These conclusions are consistent with the flow structure models discussed earlier. In deeper flows, the strength of the horseshoe vortex and associated downflow, or the analogous flow components at abutments, are related to the transverse size of the pier or abutment. Thus, the scour depth should be related to the pier or abutment size. For shallower flows (i.e., relatively long abutments), however, because the scour hole does not extend right along the upstream face of the abutment, the scour depth should be less dependent on abutment length or, in the limit, independent of it. Although an unlikely situation in practice, the scour hole at the analogous very wide vertical wall pier develops as two holes, one at each end of the "pier," as shown in Fig. 1(b). For the experiment, the pier comprised a 1-m-wide flat sheet installed centrally across a 2.4-m-wide flume with a flow depth of 50 mm. The experiment was run for 235 hours at the threshold condition for sediment movement. In spite of the very long experiment duration, the scour holes at each end of the pier did not completely merge on the central axis, as expected for a pier in a deeper flow.

Melville (1992) used the foregoing concepts to classify abutment scour. His plot of laboratory data for scour depth at wing-wall, vertical-wall, and spill-through abutments, augmented by data from Dongol (1994), is in Fig. 2(b). The original data are tabulated in Melville (1992), which also gives details of the abutment models used. The new data are given in Table 1. For the spill-through abutment models, side slopes (horizontal:vertical) of 0.5:1, 1:1, and 1.5:1 were used. More

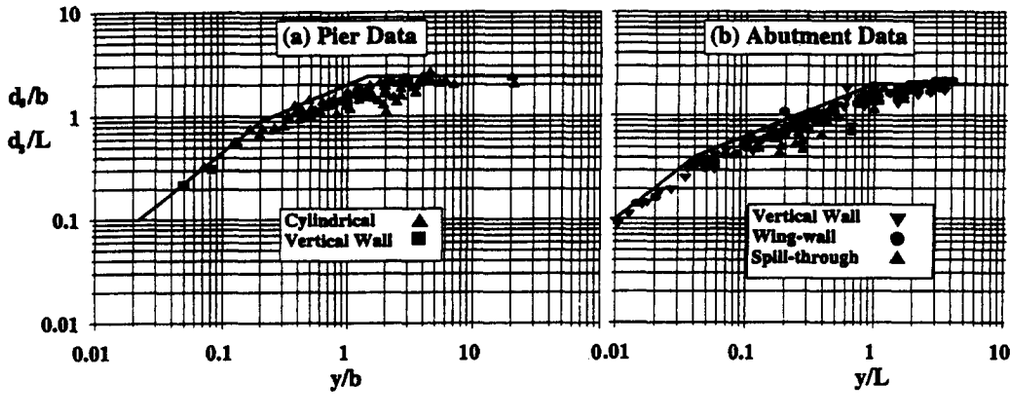

FIG. 2. Local Scour Depth Maxima at: (a) Aligned Circular Piers; (b) Aligned Vertical-Wall Abutments

TABLE 1. Abutment Scour Data by Dongol (1994)

Abutment type (1)	y (mm) (2)	L (mm) (3)	d_s (mm) V/V_c = 1 (4)	V/V_c = 2 (5)	V/V_c = 3 (6)	V/V_c = 4 (7)
Wing wall	100	150	78	—	—	—
	100	100	129	100	113	125
	200	150	182	—	—	—
	230	150	201	158	174	192
	190	100	150	130	143	140
	330	150	222	191	210	225
	350	150	219	—	—	—
	450	150	242	—	—	—
	500	150	236	—	—	—
	530	150	240	201	237	242
	600	150	242	—	—	—
	330	100	—	135	156	160
Spill through 0.5:1	250	325	272	253	265	273
	350	325	316	271	286	312
	550	325	324	283	308	325
Spill through 1:1	350	350	263	203	173	165
	150	350	175	152	256	256
	60	550	182	—	—	—
	170	550	204	—	—	—
Vertical wall	100	150	115	—	—	—
	200	150	240	—	—	—
	390	150	300	—	—	—
	250	150	270	—	—	—
	130	150	238	—	—	—
	330	150	297	231	268	273
	350	150	292	—	—	—
	500	150	304	—	—	—
	530	150	304	255	286	294
	600	150	304	—	—	—
	100	5,750	825	—	—	—
	38	5,750	365	—	—	—
	60	5,750	504	—	—	—
	38	3,750	350	—	—	—
	60	3,750	510	—	—	—
	100	3,750	720	—	—	—
	100	1,750	525	—	—	—
	60	1,750	435	—	—	—
	38	1,750	315	—	—	—
	60	4,750	524	—	—	—
	100	120	—	144	146	168
	190	120	—	163	192	190
	330	120	—	194	214	210
	230	150	—	193	246	247

than 170 data points are shown. Most of the data were obtained at the threshold condition for sediment movement and are therefore maxima for the particular foundation geometry. About 50 data points were measured by Dongol (1994) under conditions of general sediment transport on the channel bed at velocities up to those for the transition flat bed, which show slightly reduced scour depths, as expected. The latter data apply to velocity ratios, V/V_c = 1.0, 2.0, 3.0, and 4.0. V is the mean approach velocity, while V_c is the value of V at the threshold condition of sediment movement. This aspect is discussed further in the section titled "Flow Intensity." Also, the data are independent of sediment size effects (i.e., $L/d_{50} > 50$, as described later) and have been rendered independent of abutment shape by normalizing the measured scour depths with the appropriate shape factor. The shape factors used are given in Table 2 and a subsequent equation. Their derivation is discussed later. In addition, only data for uniform sediments are shown in Fig. 2(b).

TABLE 2. Shape Factors for Piers and Abutments

Foundation type (1)	Shape (2)	K_s (3)
Pier	Circular cylinder	1.0
	Round nosed	1.0
	Square nosed	1.1
	Sharp nosed	0.9
Abutment	Vertical wall	1.0
	Wing wall	0.75
	Spill through 0.5:1 (H:V)	0.6
	Spill through 1:1	0.5
	Spill through 1.5:1	0.45

The envelope curves in Fig. 2(b) define the depth-size expressions for abutments

$$K_{yL} = 2L, \quad \frac{L}{y} < 1 \tag{2a}$$

$$K_{yL} = 2\sqrt{yL}, \quad 1 < \frac{L}{y} < 25; \quad K_{yL} = 10y, \quad \frac{L}{y} > 25 \tag{2b,c}$$

The equations apply to short, intermediate length, and long abutments, respectively. According to the envelope equations, d_s increases with both y and L in the intermediate length range of abutment scour toward limiting values for the influence of L and y, as follows.

When $L/y < 1$, d_s is independent of y and the scour occurs at a short abutment. The scour process at short abutments resembles that at piers in relatively deep flows, for which it is known that there is no influence of flow depth. When $L/y > 25$, d_s is independent of L and the scour occurs at a long abutment. Kandasamy (1989) explained that, at a long abutment, part of the flow approaching the abutment is deflected parallel to the upstream abutment face and is therefore ineffective in generating downflow ahead of the abutment. The result is that the scour depth is proportionately reduced in terms of the abutment length and ultimately the scour depth becomes independent of L.

Melville (1992) pointed out that ($2b$) is similar to the well-known Laursen equation (Laursen and Toch 1956; Laursen 1958, 1962, 1963). For abutments that do not extend over the overbank region into the river channel, Laursen's equation is well approximated by

$$d_s = 1.93\sqrt{yL} \tag{3}$$

The data in Fig. 2(b) could equally well have been plotted in terms of d_s/y and L/y. Such a plot is given in Melville (1992).

Fig. 2(a) is a plot of pier scour data and is equivalent to Fig. 2(b). About 100 data for circular cylindrical piers by Chabert and Engeldinger (1956), Laursen and Toch (1956), Hancu (1971), Bonasoundas (1973), Basak (1975), Jain and Fischer (1979), Chee (1982), Chiew (1984), and Ettema (1980) are included in Fig. 2(a). The two points for a vertical-wall pier were obtained by Kwan (1984) and Kandasamy (1989), as discussed earlier. The measured scour depths at the vertical-wall pier have been adjusted to equivalent circular pier depths by dividing by the shape factor (Table 2) for a square pier. The circular pier data with low y/b were measured during this study using a 766-mm circular cylinder in flow depths y = 55, 100 mm (d_s/D = 0.33, 0.57) and a 315-mm circular cylinder with y = 52, 105 mm (d_s/D = 0.77, 0.95). These experiments, which are unlikely to be representative of actual bridge pier installations (unless debris accumulation renders the effective b larger) due to the high values of b/y, were undertaken to determine the functional relation in this range. All the data apply to uniform sediments and were obtained for flows equal to or exceeding the threshold condition for sediment movement, with most of the data applying to the threshold condition. The data shown are all independent of sediment size effects, i.e., $b/d_{50} \geq 50$, as follows.

The envelope curves shown in Fig. 2(a) define the depth-size expressions for piers

$$K_{yb} = 2.4b, \quad \frac{b}{y} < 0.7; \quad K_{yb} = 2\sqrt{yb}, \quad 0.7 < \frac{b}{y} < 5 \tag{4a,b}$$

$$K_{yb} = 4.5y, \quad \frac{b}{y} > 5 \tag{4c}$$

The equations have the same form as (2) and identify three classes of scour at bridge piers, namely scour at wide piers ($b/y > 5$), intermediate width piers ($0.7 < b/y < 5$), and narrow piers ($b/y < 0.7$). For circular piers, (4) can be written in terms of pier diameter D rather than width b. According to the envelope equations, d_s increases with both y and b in the intermediate width range of pier scour toward limiting values for the influence of b and y, as follows. When $b/y < 0.7$, d_s is independent of y and the scour occurs at a narrow pier, i.e., in a deep flow. It is acknowledged that this limit, which is equivalent to $y/b > 1.43$, is different from that normally given for the influence of flow depth. It is usually accepted that the scour depth at piers is independent of flow depth effects for $y/b > 3$–4; see, for example, Breusers et al. (1977), Ettema (1980), and Raudkivi (1986). The reason for the difference is that (4) represents envelope equations. When $b/y > 5$, d_s is independent of b and the scour occurs at a wide pier. This limit, previously unknown, is unlikely to occur in practice for bridge piers, except at long piers skewed at large angles to the flow or at piers where substantial amounts of debris have accumulated. However, it is useful in assessing scour at large caissons and other structures installed in flowing streams. Examples include offshore structures like fixed production platforms and oil storage tanks.

Flow Intensity

Local scour at bridge foundations can be classified as occurring under live-bed or clear-water conditions. Clear-water scour occurs for velocities up to the threshold velocity for general bed movement, i.e., $V/V_c \leq 1$, while live-bed scour occurs for $V/V_c > 1$. As pointed out by many researchers, including the early classic studies by Chabert and Engeldinger (1956), Laursen and Toch (1956), Laursen (1958), and Shen et al. (1966), there are significant differences between the two classes of scour and it is important to consider them separately. Under clear-water scour conditions, there is no supply of sediment to the scour hole from upstream. Clear-water conditions are typically encountered on the bed of the flood channel of a compound river channel. Under live-bed scour conditions, sediment is continuously supplied to the scour hole and the equilibrium depth is attained when there is a balance between the sediment supply and that transported out of the hole. The discussion in this section on the effects of flow velocity on scour depth highlights the differences between clear-water and live-bed scour.

The ratio V/V_c is a measure of flow intensity and determines whether grain motion occurs on the channel bed. For $V/V_c < 1$, clear-water scour conditions exist for both uniform and nonuniform sediments. If the geometric standard deviation of the particle size distribution, $\sigma_g < 1.3$, the sediment can be considered uniform and live-bed scour occurs for $V/V_c > 1$. For nonuniform sediments ($\sigma_g > 1.3$), armoring occurs on the channel bed and in the scour hole. Armor layer formation within the scour hole is known to reduce scour depths, as discussed by Raudkivi and Ettema (1977). Melville and Sutherland (1988) used the ratio V/V_a as a measure of flow intensity for scour with nonuniform sediments, where V_a marks the transition from clear-water to live-bed conditions for a sediment-transporting flow and is equivalent to V_c for uniform sediments. For nonuniform sediments, live-bed conditions pertain when $V/V_a > 1$. If $V/V_a < 1$, however, armoring of the bed occurs as scour proceeds and clear-water conditions are considered to exist.

A method to determine V_a is given in Melville and Sutherland (1988). Thus $V_a = 0.8V_{ca}$, where V_{ca} is the mean flow velocity beyond which armoring of a nonuniform sediment bed is impossible. This condition marks the coarsest or most stable armored bed for a given bed material under conditions of no sediment replenishment from upstream.

The critical velocities V_{ca} and V_c can be determined from the logarithmic form of the velocity profile

$$\frac{V_c}{u_{*_c}} = 5.75 \log\left(5.53\frac{y}{d_{50}}\right); \quad \frac{V_{ca}}{u_{*_{ca}}} = 5.75 \log\left(5.53\frac{y}{d_{50a}}\right) \tag{5a,b}$$

where u_{*_c} = critical shear velocity based on the d_{50} size; $u_{*_{ca}}$ = critical shear velocity for the d_{50a} size; and d_{50a} = median armor size. The shear velocities are determined using the Shields diagram for the respective sizes. A useful approximation to the Shields diagram for quartz sediments in water at 20°C is

$$u_{*_c} = 0.0115 + 0.0125d^{1.4}, \quad 0.1 \text{ mm} < d < 1 \text{ mm} \tag{6a}$$

$$u_{*_c} = 0.0305d^{0.5} - 0.0065d^{-1}, \quad 1 \text{ mm} < d < 100 \text{ mm} \tag{6b}$$

where u_{*_c} (or $u_{*_{ca}}$) is in m/s and d (=d_{50} or d_{50a}) is in mm.

The particle size d_{50a} is found using an empirical expression given by Chin (1985)

$$d_{50a} = \frac{d_{\max}}{1.8} \tag{7}$$

where $d_{\max}$ = maximum particle size and is determined from the particle size distribution.

Dongol (1994) conducted an extensive series of experiments of the effect of flow velocity on abutment scour depth under

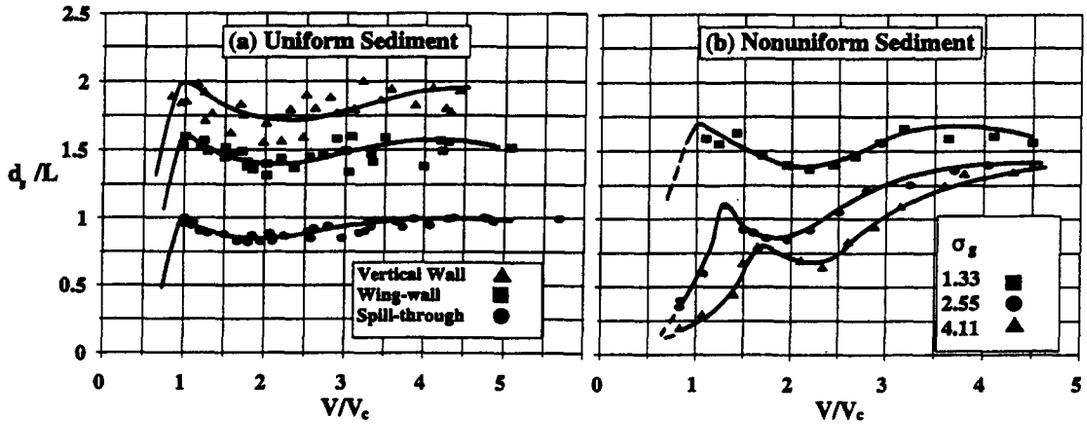

FIG. 3. Effect of Flow Intensity on Local Scour Depths at Abutments in: (a) Uniform; (b) Nonuniform Sediments

live-bed conditions for both uniform and nonuniform sediments. His data complement the studies by Chiew (1984) and Baker (1986) of live-bed scouring at bridge piers in uniform and nonuniform sediments, respectively. Melville and Sutherland (1988) used Chiew's and Baker's data to define the flow intensity factor, K_I, for pier scour. Dongol's data are used next to define K_I for abutments.

Some of Dongol's (1994) data for live-bed scour at abutments in a uniform sediment of median size 0.9 mm are shown in Fig. 3(a). The equilibrium live-bed scour depth fluctuates about an average value due to the passage of bed forms past the scour hole. The scour depths shown in Fig. 3(a) are average equilibrium values. The data for the vertical-wall (L = 150 mm) and spill-through (side slopes = 0.5:1, L = 325 mm at middepth) abutment models were measured in a 1,500-mm-wide flume with flow depths ranging from 230 to 550 mm. The wing-wall (L = 120 mm) model data were obtained in the same flume with flow depths ranging from 100 to 330 mm. The trends shown are typical of the complete set of data given by Dongol (1994). For each abutment type, experiments were conducted for several values of relative flow depth y/L, within the intermediate length range. Following the foregoing concepts, the data for different values of y/L have been adjusted by dividing by $(y/L)^{0.5}$, thus rendering them independent of flow depth effects. The adjustment has the expected effect of collapsing the data for each abutment type, as shown in Fig. 3(a). The abutment shape factors discussed later in this paper were derived by Dongol by comparing data for each abutment type based on plots similar to that in Fig. 3(a).

The trends in the data in Fig. 3(a) are the same as those evident in pier scour data. Under clear-water conditions, the maximum scour depth occurs at V_c. The scour depth is called the threshold peak. For $V/V_c > 1$ under live-bed conditions, d_s initially reduces with increasing flow velocity, reaches a minimum value, and then increases again toward a second maximum. The second maximum occurs at about the transition flat-bed stage of sediment transport on the channel bed and is termed the live-bed peak. Chee (1982), Chiew (1984), and Melville and Sutherland (1988) discussed the scour depth variations under live-bed conditions in terms of the size and steepness of the bed features pertaining at particular flow velocities. They explained that the shorter and higher the bed forms, the lesser the observed scour depth because the flow within the scour hole is incapable of removing the sediment supplied with the passage of a given bed form prior to the arrival of the next bed form. The live-bed peak occurs at about the transition flat-bed condition when the bed forms are very long and of negligible height.

A typical set of Dongol's (1994) data for scour at nonuniform sediments is given in Fig. 3(b). The data were obtained in a 440-mm-wide flume using a wing-wall abutment model with L = 100 mm and wall angles of 45°. The data shown were obtained with a flow depth of 330 mm, although Dongol made measurements for flow depths of 100 and 210 mm as well. The median size of the three sediments used (σ_g = 1.33, 2.55, and 4.11) was 0.9 mm. The trend in the data is the same as that for scour at piers in nonuniform sediments. Typical pier data are given by Baker (1986) and Melville and Sutherland (1988). For nonuniform sediments, the scour depth maxima are termed the armor peak and the live-bed peak. For velocities less than the armor peak velocity V_a, armoring occurs and the scour depth is limited accordingly. Beyond V_a, the armoring diminishes and live-bed conditions pertain. The live-bed peak occurs at the transition flat-bed condition when all particle sizes in the nonuniform sediment are in motion. At the live-bed peak, the scour depth is reasonably constant irrespective of σ_g.

For nonuniform sediments, Melville and Sutherland (1988) plotted data showing the influence of flow intensity on scour depth at piers in terms of the velocity parameter $[V - (V_a - V_c)]/V_c$. This parameter has the effect of aligning the armor peak for nonuniform sediments with the threshold peak for uniform sediments. For uniform sediments, $V_a \equiv V_c$ and $[V - (V_a - V_c)]/V_c \equiv V/V_c$. The velocity parameter incorporating V_a largely accounts for the effects of sediment gradation as well as those of flow velocity, although the smaller values of scour depth at $[V - (V_a - V_c)]/V_c \approx 1$, as σ_g increases, remain.

Scour depth data for piers and abutments in uniform and nonuniform sediments are given in Figs. 4 and 5. In the figures, the flow intensity factor K_I is the ratio of the scour depth at a particular flow velocity to that at either the threshold peak or the live-bed peak. The data for uniform sediments are normalized with the scour depth at the threshold peak, except for the few data for ripple-forming sediments (d_{50} < 0.6 mm) for which the live-bed peak is used. Ettema (1980) showed that scour depths near the threshold peak for ripple-forming sediments were reduced due to the formation of ripples. For ripple-forming sediments, the live-bed peak exceeds the threshold peak. The data for nonuniform sediments are normalized with the scour depth at the live-bed peak.

Fig. 4(a) includes about 200 data points for equilibrium scour depth at circular piers in uniform sediments derived from several studies. The number of points plotted and the range of values of D, y, d_{50}, and V/V_c for each study are given in Table 3. Scour depth data at piers in nonuniform sediments by Chiew (1984) and Baker (1986) are shown in Fig. 5(a). For the former, D = 31.75 mm, y = 170 mm, d_{50} = 0.6, 0.8, and 1.45 mm, and σ_g = 1.3, 2.0, 2.8, 4.3, and 5.5. For the latter, D = 45 mm, y = 170, 270 mm, d_{50} = 0.6 mm, and σ_g = 1.3, 2.3, 2.9, 4.4, and 5.2.

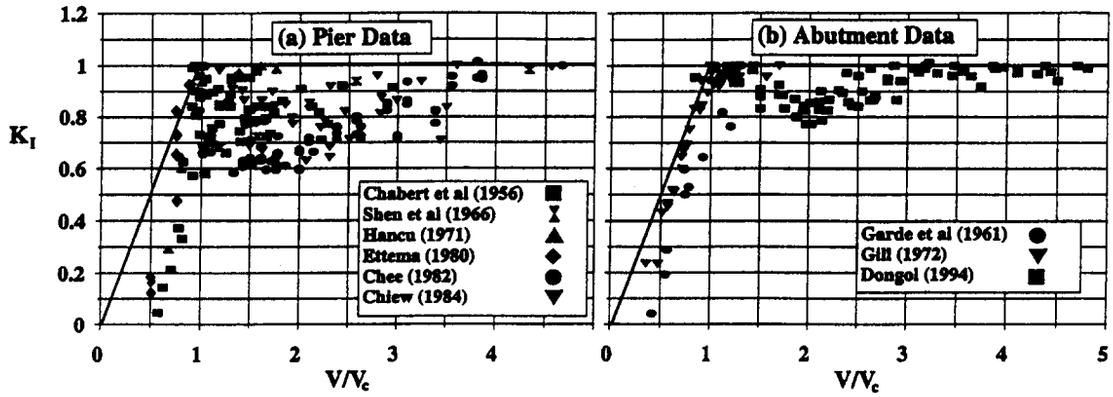

FIG. 4. Flow Intensity Factor for: (a) Piers; (b) Abutments, Uniform Sediment Data

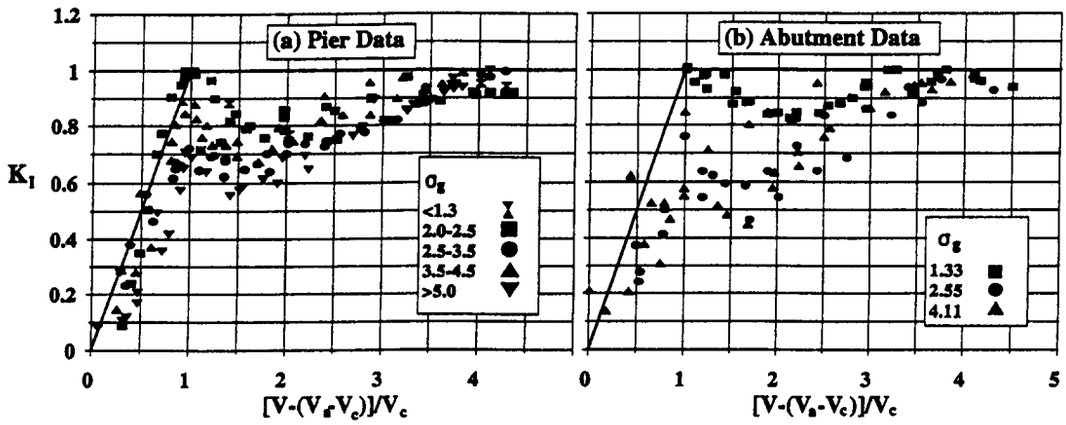

FIG. 5. Flow Intensity Factor for: (a) Piers; (b) Abutments, Nonuniform Sediment Data

TABLE 3. Details of Pier and Abutment Data in Fig. 4

Source (1)	Pier or abutment type (2)	Number of points (3)	D or L (mm) (4)	y (mm) (5)	d_{50} (mm) (6)	V/V_c (7)
Chabert and Engeldinger (1956)	Circular cylindrical pier	54	150	100–350	1.5, 3	0.57–2.94
Shen et al. (1966)		6	150	115	0.24	1.19–5.14
Hancu (1971)		10	130	100	2	0.68–1.76
Ettema (1980)		15	50.8	600	0.38–5.35	0.5–0.95
Chee (1982)		76	51–102	100	0.24–1.40	1.02–5.24
Chiew (1984)		40	32–45	170–210	0.24–3.2	0.89–4.56
Garde et al. (1961)	Vertical wall abutment	11	102	49–216	1	0.42–1.3
Gill (1972)	Vertical wall abutment	30	102–305	20–100	0.9, 1.52	0.36–1.69
Dongol (1994)	75° wing-wall abutment	13	120	330	0.9	1.03–4.3
	45° wing-wall abutment	13	100	330	0.9	1.1–4.5
	0.5:1 spill-through abutment	11	325 at middepth	550	0.9	1.01–4.8
	45° wing-wall abutment	12	150	530	0.9	1.01–4.7
	Vertical wall abutment	13	150	530	0.9	0.83–4.43
	1:1 spill-through abutment	15	350 at middepth	350	0.9	1.02–3.74

Fig. 4(b) includes about 120 data points for scour at abutments in uniform sediments derived from several studies. The number of points included, the types of abutment model, and the range of values of L, y, d_{50}, and V/V_c for each study are given in Table 3. The data by Dongol (1994) were divided into groups of equal L and y and normalized with the largest scour depth, which occurred at the threshold velocity, as described earlier. Gill's (1972) data were divided into groups of equal L and y and normalized with the largest scour depth, which occurred typically at $V/V_c > 1$. The reason for the larger scour depth occurring under live-bed conditions rather than at the threshold condition is that Gill (1972) recorded the maximum scour depth, i.e., including fluctuations due to bed forms, rather than the average equilibrium depth. Chiew (1984) pointed out that it is better to measure the local scour depth under live-bed conditions as a temporal average depth because the component due to bed forms is independent of the foundation size. The Garde et al. (1961) data were recorded for varying y and V. One set of their data is plotted in Fig. 4(b). The data shown were normalized with the maximum scour depth, which occurred at $V/V_c = 1.3$. For that experiment, Garde et al. (1961) observed very little sediment transport, while for the other data shown they observed no or very little sediment transport. For the aforementioned reasons, it is considered appropriate to include the data by Garde et al. (1961) and Gill (1972) in Fig. 4(b).

Dongol's (1994) data for local scour depth at a 45° wing-wall abutment founded in nonuniform sediments are shown in Fig. 5(b). For all the data, L = 100 mm and d_{50} = 0.9 mm. Flow depths y = 100, 210, and 330 mm were used.

The envelope curves drawn in Figs. 4 and 5 define the flow intensity factor, K_I, and are given by

$$K_I = \frac{V - (V_a - V_c)}{V_c}, \quad \frac{V - (V_a - V_c)}{V_c} < 1 \qquad (8a)$$

$$K_I = 1, \quad \frac{V - (V_a - V_c)}{V_c} \geq 1 \qquad (8b)$$

These equations envelop nearly all the data for piers and abutments for both uniform and nonuniform sediments. The scatter of the data, particularly for $[V - (V_a - V_c)]/V_c$ or V/V_c in the 1–3 range is considerable. For uniform sediments, the scatter arises because of the supply of sediment into the scour hole as bed forms propagate past the bridge foundation. For nonuniform sediments, the scatter is due to sediment supply with bed-form propagation and the effects of armoring. In spite of the scatter, it is considered appropriate to use (8*b*) for design purposes, because of the uncertainties associated with design flood prediction and the possibility that high values of the flow velocity parameter could occur. Eq. (8*a*) is appropriate for design purposes where clear-water scour conditions are known to exist, for example in the flood channel where the depth and velocity of flow are often much reduced.

Several equations for estimation of local scour depth at bridge foundations, including those recommended in Richardson et al. (1993), do not distinguish correctly between clear-water and live-bed scour. The shortcoming is represented by a strong dependence on V (or the Froude number based on V) in live-bed scour relations. The trends evident in Figs. 4 and 5 show that d_s is approximately proportional to flow velocity under clear-water conditions but is largely independent of flow velocity under live-bed conditions. This feature was recognized in the pioneering study by Laursen and Toch (1956), who stated in their conclusions: "Insofar as the equilibrium depth of scour in a model is concerned, the velocity of flow, the sediment size, and the rate of sediment transport do not need to be scaled. Exactly the same depth of scour should result in the model, no matter what velocity or sediment is used, as long as there is general bed-load movement and the Froude number is everywhere less than unity."

Sediment Size

Ettema (1980) for clear-water flows and Chiew (1984) for live-bed scour, defined the influence of sediment size on scour depth at circular piers for uniform sediments. Their data show that d_s increases with the relative sediment size (b/d_{50}) up to $b/d_{50} = 50$. For $b/d_{50} > 50$, d_s is independent of the sediment size. Ettema explained that the reductions in scour depth for relatively large sediments were due to large particles impeding the erosion process at the base of the scour hole and dissipating some of the flow energy in the erosion zone. The pier data by Ettema and Chiew are plotted in Fig. 6(a) in terms of the sediment size multiplying factor, K_d, which is defined generally as the ratio of the scour depth for a particular W/d_{50} to that for $W/d_{50} \geq 50$. The pier data are augmented with abutment scour data by Dongol (1994), plotted in terms of L/d_{50} rather than b/d_{50}. The latter were obtained at the threshold condition for sediment movement using a vertical-wall abutment model and uniform sediments. All the data shown in Fig. 6(a) were obtained for relatively deep flows and thus have no influence of flow depth. The plot shows that the influence of relative sediment size on scour depth is the same for both piers and abutments, although more data are needed to confirm this finding for abutments. Because the condition $L/d_{50} < 50$ is unlikely in practice, it is considered that the few abutment data shown in Fig. 6(a) are adequate for preliminary definition of K_d for design purposes.

The envelope curves in Fig. 6(a) define the sediment size factor for design purposes and have the following equations:

$$K_d = 0.57 \log\left(2.24 \frac{W}{d_{50}}\right), \quad \frac{W}{d_{50}} \leq 25; \quad K_d = 1.0, \quad \frac{W}{d_{50}} > 25 \qquad (9a,b)$$

where $W \equiv b$ for piers; and $W \equiv L$ for abutments. These equations are identical to those given in Melville and Sutherland (1988).

The data used to determine (9) apply to uniform sediments. Consideration is now directed to sediment size effects for nonuniform sediments, which are characterized by channel bed armoring as discussed earlier. In Fig. 6(b), data for nonuniform sediments are plotted for different values of the velocity parameter $[V - (V_a - V_c)]/V_c$. The data are plotted in terms of b/d_{50a} or L/d_{50a} because the median size of the armor layer is considered to be the characteristic sediment size. Thus for nonuniform sediments, (9) is expressed in terms of W/d_{50a}. Fig. 6(b) includes data by Ettema (1980), Chiew (1984), and Baker (1986) for piers and Dongol (1994) for abutments. The former were obtained at the value $[V - (V_a - V_c)]/V_c = 1.0$, while those from the other authors were obtained for a range of flow velocities, including $[V - (V_a - V_c)]/V_c = 1.0$, 2.0, 3.0, and 4.0, as shown. With two minor exceptions, the data lie within the envelope curves for uniform sediments. The agreement between the data and the envelope curves improves with increasing velocity, consistent with the trends evident in Fig. 3(b).

Pier and Abutment Shape

Various types and shapes of piers and abutments are depicted in Fig. 7. Definition sketches for the effects of floating debris at bridge piers and for channel geometry effects at bridge abutments are shown also.

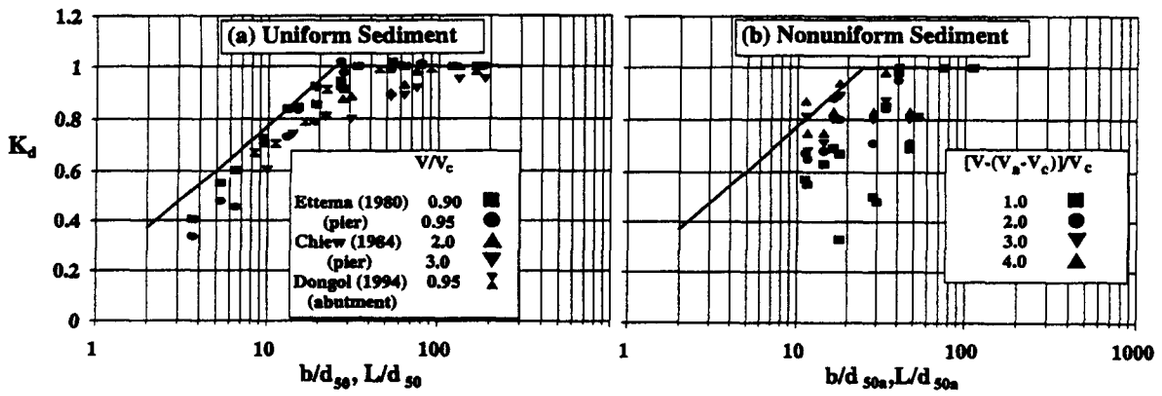

FIG. 6. Sediment Size Factor for Piers and Abutments: (a) Uniform Sediment Data; (b) Nonuniform Sediment Data

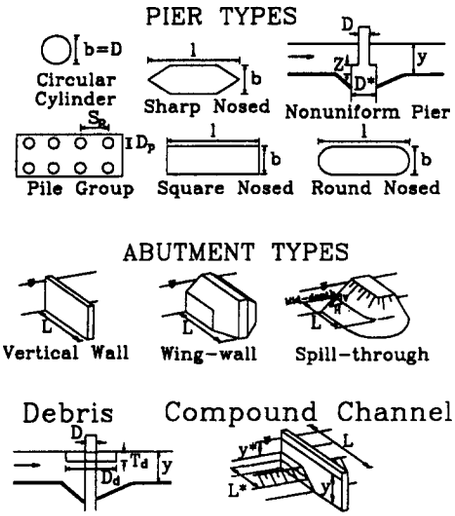

FIG. 7. Geometric Classification of Piers and Abutments for Scour Purposes

To be consistent with (2) and (4), circular cylindrical piers and vertical-wall abutments are selected as the primary shapes and, therefore, they have shape factor $K_s = 1$. Shape factors for other pier and abutment types are given in Table 2. Several studies of scour at bridge piers give values of shape factors including those by Laursen and Toch (1956), Larras (1963), Maza Alvarez (1968), and Richardson et al. (1993). Melville and Sutherland (1988) give a selection of K_s values for piers, taken from the earlier studies. The values of K_s for circular cylindrical piers and square, sharp, and round-nosed piers given in Table 2 are taken from Richardson et al. (1993). For these shapes, K_s is reasonably constant, indicating that shape effects are relatively insignificant. The K_s values for piers in Table 2 apply only to piers aligned with the flow.

Raudkivi and Sutherland (1981) give values, based on a study by Hannah (1978), of shape factor for piled foundations where the pile cap is clear of the water surface. The K_s values are shown in Table 4 for a single row and a double row of piles in terms of the approach flow angle, θ, pile diameter, D_p, and pile spacing, S_p. The former also apply to a pier comprising a row of cylinders. The values shown include pier alignment effects and shape effects, i.e., they represent $K_s K_\theta$.

Melville and Raudkivi (1994) undertook a systematic investigation of scour at a nonuniform cylindrical pier, i.e., a circular cylindrical pier (size D) founded on a larger cylinder (size D^*). The results of the study apply to nonuniform piers, including piers founded on slab footings, where the footing is above or within the scour hole. If the footing is below the bottom of the scour hole, the pier is treated as a uniform pier of size D because the footing does not affect the scour. Melville and Raudkivi (1994) used the data to show that the scour depth at the equivalent uniform pier of diameter D_e was always less than that given by the method in Melville and Sutherland (1988). The equation for D_e is given in terms of the geometric variables shown in Fig. 7. The level of the top of the footing, Z, is positive as shown, but is negative if the top of the footing is below bed level

$$D_e = D\left(\frac{y - Z}{y + D^*}\right) + D^*\left(\frac{D^* + Z}{D^* + y}\right) \tag{10}$$

Similarly, for the effects of floating debris at bridge piers, Melville and Dongol (1992) defined an equivalent uniform diameter for which scour depths were always less than those given by the Melville and Sutherland (1988) method. The equation for D_e to account for debris effects is

$$D_e = \frac{0.52T_dD_d + (y - 0.52T_d)D}{y} \tag{11}$$

where T_d and D_d = thickness and diameter of the floating debris raft, as shown in Fig. 7.

The values given in Table 2 for shape factor at bridge abutments are those evaluated by Dongol (1994), as discussed, and given by Melville (1992). The K_s values reveal that considerable scour depth reductions are afforded by streamlining the shape of abutment for shorter abutments. Because shape effects are unimportant at longer abutments, Melville (1992) recommended using the adjusted shape factor, K_s^*, as follows:

$$K_s^* = K_s, \quad \frac{L}{y} \le 10 \tag{12a}$$

$$K_s^* = K_s + 0.667(1 - K_s)\left(0.1\frac{L}{y} - 1\right), \quad 10 < \frac{L}{y} < 25 \tag{12b}$$

$$K_s^* = 1.0, \quad \frac{L}{y} \ge 25 \tag{12c}$$

Pier and Abutment Alignment

Melville (1992) plotted data for the effects of abutment alignment with respect to the flow. The data were derived from studies by Ahmad (1953), Laursen (1958), Sastry (1962), Zaghloul (1983), Kwan (1984), and Kandasamy (1985). The data were analyzed in terms of the scour depth at an abutment aligned across the flow, i.e., having angle of alignment $\theta = 90°$, for which $K_\theta = 1.0$. For $\theta < 90°$, the abutment is pointed downstream and vice versa. Melville (1992) fitted an envelope curve to the data. The values given in Table 5 are derived from the envelope curve. Clearly, abutment alignment has a relatively insignificant effect on the depth of scour. Note that because L is defined as the projected length of abutment (measured perpendicular to the flow), abutments of different alignment extending the same lateral distance into the channel have different actual lengths.

Melville (1992) recommended that the alignment factor be applied only to longer abutments and gave the adjusted alignment factor K_θ^* as

$$K_\theta^* = K_\theta, \quad \frac{L}{y} \ge 3 \tag{13a}$$

$$K_\theta^* = K_\theta + (1 - K_\theta)\left(1.5 - 0.5\frac{L}{y}\right), \quad 1 < \frac{L}{y} < 3 \tag{13b}$$

$$K_\theta^* = 1.0, \quad \frac{L}{y} \le 1 \tag{13c}$$

The Laursen and Toch (1956) curve for flow alignment effects at bridge piers is widely used. Values of the alignment factor for piers given in Richardson et al. (1993) are reasonably consistent with the Laursen and Toch (1956) curve and are included in Table 5 for different values of the pier length to width ratio, l/b. The angle of alignment for piers is the angle

TABLE 4. Multiplying Factors ($K_s K_\theta$) for Pile Groups

Type (1)	S_p/D_p (2)	$K_s K_\theta$		
		$\theta < 5°$ (3)	$\theta = 5$–$45°$ (4)	$\theta = 90°$ (5)
Single row	2	1.12	1.40	1.20
	4	1.12	1.20	1.10
	6	1.07	1.16	1.08
	8	1.04	1.12	1.02
	10	1.00	1.00	1.00
Double row	2	1.50	1.80	—
	4	1.35	1.50	—

TABLE 5. Values of Flow Alignment Factor

Foundation type (1)		K_θ (°) θ = 0 (2)	15 (3)	30 (4)	45 (5)	60 (6)	90 (7)	120 (8)	150 (9)
Pier	l/b = 4	1.0	1.5	2.0	2.3	—	2.5	—	—
	8	1.0	2.0	2.75	3.3	—	3.9	—	—
	12	1.0	2.5	3.5	4.3	—	5.0	—	—
Abutment		—	—	0.9	—	0.97	1.0	1.06	1.08

between the flow direction and the major axis of the pier. For $l/b > 12$, Richardson et al. (1993) recommend that the values for $l/b = 12$ should be used as a maximum. Clearly flow alignment effects can be very important at bridge piers with values up to $K_\theta = 5$, which is possible for large θ. The significance of flow alignment effects at piers means single circular cylindrical piers ($K_\theta = 1$ irrespective of θ) or piers comprising a single row of circular columns ($K_s K_\theta < 1.20$ for all θ and $S_p/D_p > 4$) are to be preferred to other pier types where significant flow angles can occur.

Channel Geometry

Channel geometry effects are unimportant at bridge piers, as long as the velocity and depth of flow used represent the flow approaching the pier under consideration. Thus, the channel geometry factor for piers is taken as $K_G = 1.0$.

A systematic investigation of the effect of approach channel geometry on the scour at an abutment sited in a compound channel comprising flood and main channels is presented by Melville and Ettema (1993) and Melville (1995). The study is limited to the case of an abutment spanning the flood channel and extending into the main channel. The data are used to define the channel geometry factor, K_G, which is defined as the ratio of the depth of scour at the given abutment sited in the compound channel to that at the same abutment sited in a rectangular channel of the same width and depth equal to the main channel depth, termed the corresponding rectangular channel. Melville and Ettema (1993) derived the following equation for K_G:

$$K_G = \sqrt{1 - \frac{L^*}{L}\left[1 - \left(\frac{y^*}{y}\right)^{5/3}\frac{n}{n^*}\right]} \tag{14}$$

where L^* = width of the flood channel and is equivalent to the (projected) length of abutment spanning the flood channel; y^* = depth of flow in the flood channel; and n and n^* = Manning roughness coefficients for the main and flood channels. A schematic diagram is included in Fig. 7. Eq. (14) is based on the assumption that $d_s \propto \sqrt{A}$, where A represents the area of flow obstructed by the abutment. For a rectangular channel $A = Ly$ as shown by (2*b*). For a compound channel, A comprises areas of flood channel (based on L^* and y^*) and main channel (based on L, L^*, and y), weighted according to the respective flow velocities, the latter being related by the Manning equation. K_G is expressed as the ratio of scour depths in the compound and the corresponding rectangular channels. For an abutment spanning a shallow and rough flood channel and extending a short distance into the main channel, (14) shows that significant scour depth reductions are observed compared to the scour depth at the same abutment in a rectangular channel. For example, for $L^*/L = 0.9$, $y^*/y = 0.2$, and $n^*/n = 0.3$, the scour depth is about one-third of that in the corresponding rectangular channel.

The only other known data for compound channel geometry effects are given by Sturm and Janjua (1994). They considered abutments situated in the flood channel, but set well back from the edge of the main channel. Using their data, Melville (1995) showed that such cases can be reasonably well represented by considering only the flow in the flood channel, i.e., ignoring the main channel flow. This concept is illustrated in the examples presented later.

DESIGN RECOMMENDATIONS

The design method is based on laboratory data for circular cylindrical piers (D) and vertical wall abutments (L). The equilibrium local scour depth is estimated using (1), where the Ks are given by the empirical relations presented earlier. Temporal effects are not incorporated in (1) because no adequate time-scaling parameter for local scour is available. Thus, the method is incapable of predicting the lesser scour depths that can occur if, for example, the design flood duration is shorter than that required to develop the equilibrium scour depth. This limitation is more serious under clear-water conditions, which can occur at bridge foundations sited in a flood plain. For circular piers or vertical-wall abutments oriented perpendicular to the flow, K_{yw} (m) represents the maximum possible scour depth. Values of K_I, K_d, and K_G are always ≤1.0 and the effect of each of these factors is to reduce the scour depth given by K_{yw}. Scour depths at aligned square-nosed piers can be up to 10% higher than given by K_{yb}. For skewed noncircular piers, significantly larger scour depths than given by K_{yb} can occur (i.e., $K_\theta \rightarrow 5$). For abutments oriented obliquely to the channel, slightly larger scour depths than given by K_{yL} can occur (i.e., $K_\theta \rightarrow 1.1$). The design method is summarized in the flowchart in Fig. 8. Two examples of application of the design method are presented next. Each example is composed to illustrate several different aspects of the design method and is therefore not necessarily representative of an actual bridge crossing.

Example One

Find the pier and abutment scour depths at the bridge crossing shown in Fig. 9(a). Mean velocities are 1.0 and 0.4 m/s in the main and flood channels, respectively, and the sediment is uniform, $d_{50} = 1$ mm. Abutment A1, which spans the flood channel and extends into the main channel, is located in a compound channel in terms of scour estimation. Abutment A2 is considered to be situated in a rectangular channel having flood channel flow velocity (V^*) and depth (y^*); it is assumed that the scour is not affected by the main channel flow. The implication is that the abutment extends a relatively short distance across the flood channel. The flow velocity and depth for pier P1 are the main channel velocity and depth, while the flood channel velocity and depth are considered appropriate for pier P2. Pier P1 is nonuniform as shown. However, pier P2 is considered to be uniform for scour estimation purposes because the top elevation of the lower pier is assumed to be below the base of the scour hole. This assumption is confirmed by the calculations.

The given data are as follows:

Flow: $V = 1.0$ m/s, $V^* = 0.4$ m/s, $y = 8$ m, $n = 0.020$
Sediment: $d_{50} = 1$ mm, $\sigma_g = 1.3$
Foundation geometry:
- A1: Wing-wall abutment, $L = 120$ m, $\theta = 60°$
- A2: Wing-wall abutment, $L = 10$ m, $\theta = 120°$
- P1, P2: Nonuniform, square-nosed piers—upper pier: l = 8 m, $b = 2$ m, $\theta = 15°$; lower pier: $l = 9$ m, $b = 3$ m, $\theta = 15°$

Channel geometry:
- A1: $L^* = 110$ m, $y^* = 2$ m, $n^* = 0.040$

The initial task is to determine the velocity parameters in the main and flood channels. For the main channel, (6*a*) gives $u_{*c} = 0.024$ m/s and then $V_c = 0.64$ m/s from (5*a*). Thus V/V_c

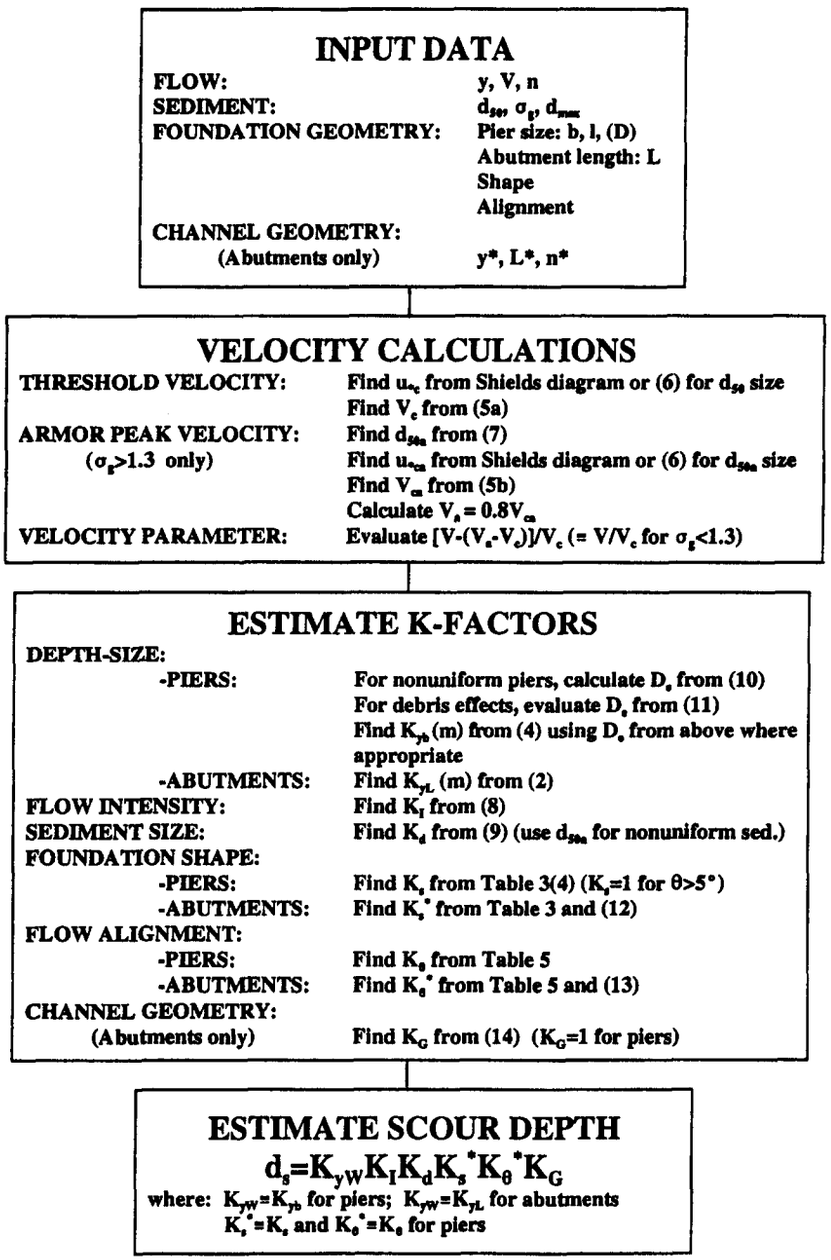

FIG. 8. Flowchart of Method for Scour Depth Estimation

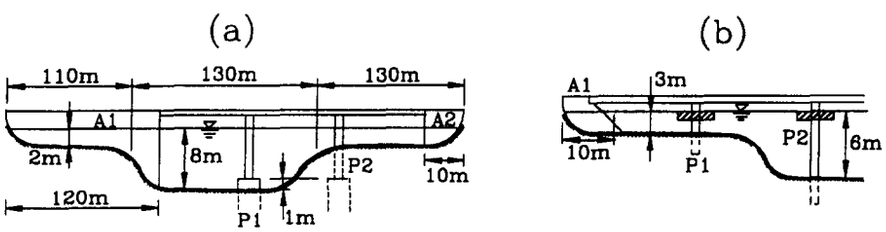

FIG. 9. Definition Sketches for Examples of Scour Depth Estimation

= 1.56 and live-bed scour occurs. Similarly, for the flood channel, $V_c^* = 0.56$ m/s, $V^*/V_c^* = 0.72$ and thus clear-water scour occurs.

The next step is to evaluate the K-factors, as follows:

Depth size:
For A1, $Ly = 120/8 = 15$ and $K_{yL} = 62.0$ m from (2*b*)
For A2, $L/y = 10/2 = 5$ and $K_{yL} = 8.94$ m from (2*b*)
For P1, $D \equiv 2$ m, $D^* \equiv 3$ m, $Z = 1$ m, and $D_e = 2.36$ m from (10); thus, $b/y \equiv D_e/y = 2.36/8 = 0.30$ and $K_{yb} = 5.7$ m from (4*a*)
For P2, $b/y = 2/2 = 1.0$ and $K_{yb} = 4.0$ m from (4*b*)

Flow intensity:
For A1 and P1, $V/V_c = 1.56$ and $K_I = 1.0$ from (8*b*)
For A2 and P2, $V^*/V_c^* = 0.72$ and $K_I = 0.72$ from (8*a*)

Sediment size:
For A1 and A2, $L/d_{50} > 25$ and $K_d = 1.0$ from (9*b*)
For P1 and P2; $b/d_{50} > 25$ and $K_d = 1.0$ from (9*b*)

Foundation shape:
For A1, $K_s = 0.75$ from Table 2, $L/y = 15$, and $K_s^* = 0.833$ from (12*b*)
For A2, $K_s = 0.75$ from Table 2, $L/y = 5$, and $K_s^* = 0.75$ from (12*a*)
For P1 and P2, $K_s \equiv K_s^* = 1.0$ because $\theta > 5°$
Foundation alignment:
For A1, $\theta = 60°$, $K_\theta = 0.97$ from Table 5, $L/y = 15$, and $K_\theta^* = 0.97$ from (13*a*)
For A2, $\theta = 120°$, $K_\theta = 1.06$ from Table 5, $L/y = 5$, and $K_\theta^* = 1.06$ from (13*a*)
For P1 and P2, $l/b = 8/2 = 4$, $\theta = 15°$, and $K_\theta \equiv K_\theta^* = 1.5$ from Table 5
Channel geometry:
For A1, $K_G = 0.36$ from (14)
For A2, P1, and P2, $K_G = 1$
The final step is to estimate the depth of scour from (1)
For A1, $d_s = 18.0$ m
For A2, $d_s = 5.1$ m
For P1, $d_s = 8.5$ m
For P2, $d_s = 4.3$ m

Example Two

Find the pier and abutment scour depths at the bridge crossing shown in Fig. 9(b). Mean velocities are 3.0 and 1.5 m/s in the main and flood channels, respectively, and the sediment is nonuniform. Abutment A1 is considered to be situated in a rectangular channel having flood channel flow velocity (V^*) and depth (y^*); it is assumed that the abutment is set back a relatively large distance from the main channel. The flow velocity and depth for pier P1 are the flood channel velocity and depth, while the main channel velocity and depth are considered appropriate to pier P2. Both piers are subject to debris contamination as shown.

The given data are:

Flow: $V = 3.0$ m/s, $V^* = 1.5$ m/s, $y = 6$ m, $n = 0.020$
Sediment: $d_{50} = 12$ mm, $d_{\max} = 100$ mm, $\sigma_g = 4$
Foundation geometry:
A1: Spill-through abutment (1:1), $L = 10$ m, $\theta = 90°$
P1, P2: Circular piers $D = 1$ m, $D_d = 5$ m, $T_d = 1.5$ m, $\theta = 0°$

The initial task is to determine the velocity parameters in the main and flood channels. For the main channel, (6*b*) gives $u_{*_c} = 0.105$ m/s and then $V_c = 2.08$ m/s from (5*a*). Also, $d_{50a} = 55.6$ mm from (7), $u_{*_{ca}} = 0.227$ m/s from (6*b*), $V_{ca} = 3.63$ m/s from (5*b*), and $V_a = 0.8V_{ca} = 2.90$ m/s. Thus $[V - (V_a - V_c)]/V_c = 1.05$ and live-bed scour occurs. Similarly for the flood channel, $V_c^* = 1.90$ m/s, $V_a^* = 2.58$ m/s $[V^* - (V_a^* - V_c^*)]/V_c^* = 0.43$ and clear-water scour occurs.

The next step is to evaluate the K-factors, as follows:

Depth size:
For A1, $L/y = 10/3 = 3.33$ and $K_{yL} = 11.0$ m from (2*b*)
For P1, $D_e = 2.04$ m from (11); thus, $D_e/y = 2.04/3 = 0.68$ and $K_{yb} = 4.9$ m from (4*a*)
For P2, $D_e = 1.52$ m from (11); thus, $D_e/y = 1.52/6 = 0.25$ and $K_{yb} = 3.65$ m from (4*a*)
Flow intensity:
For A1 and P1, $[V^* - (V_a^* - V_c^*)]/V_c^* = 0.43$ and $K_I = 0.43$ from (8*a*)
For P2, $[V - (V_a - V_c)]/V_c = 1.05$ and $K_I = 1.0$ from (8*b*)
Sediment size:
For A1, $L/d_{50a} > 25$ and $K_d = 1.0$ from (9*b*)
For P1 and P2, $D_e/d_{50a} > 25$ and $K_d = 1.0$ from (9*b*)
Foundation shape:
For A1, $K_s = 0.5$ from Table 2, $L/y = 3.33$, and $K_s^* = 0.5$ from (12*a*)
For P1 and P2, $K_s \equiv K_s^* = 1.0$
Foundation alignment:
For A1, $\theta = 90°$, $K_\theta = 1.0$ from Table 5, $L/y = 3.33$, and $K_\theta^* = 1.0$ from (13*a*)
For P1 and P2, $K_\theta \equiv K_\theta^* = 1.0$ because $\theta = 0°$
Channel geometry:
For A1, P1, and P2, $K_G = 1.0$

The final step is to estimate the depth of scour from (1):
For A1, $d_s = 2.4$ m
For P1, $d_s = 2.1$ m
For P2, $d_s = 3.65$ m

CONCLUDING REMARKS

The equilibrium depth of local scour at bridge piers or abutments, collectively termed bridge foundations, can be estimated for design purposes using (1) with the aid of the flowchart in Fig. 8. Eq. (1) comprises empirically determined expressions for the various factors that can affect the equilibrium local scour depth. The expressions envelop the available laboratory data, rendering them inherently conservative, at least at the laboratory scale. The view that reliable field data are needed to test scour depth estimators has been expressed often. Such data would be valuable for assessing the new method at the prototype scale.

K_{yL} (m) and K_{yb} (m), which are given by (2) and (4), represent the maximum possible scour depth that can develop at aligned vertical-wall abutments and circular cylindrical piers, respectively. The maximum possible scour depth is that which occurs in the absence of the influences of flow velocity, sediment size and gradation, and channel geometry. According to (2) and (4), there are three ranges of scour depth dependence: $d_s \propto W$ for very short abutments and very narrow piers, $d_s \propto (yW)^{0.5}$ for intermediate size foundations, and $d_s \propto y$ for very long abutments and very wide piers.

For aligned piers, the scour depth can be increased up to $1.1K_{yb}$ depending on the pier shape. For skewed piers, significant increases of scour depth up to $5K_{yb}$ can occur, while for skewed abutments, the scour depth can be up to $1.1K_{yL}$. The remaining K-factors all have the effect of reducing the scour depths given by K_{yb} or K_{yL}.

ACKNOWLEDGMENTS

Appreciation is recorded for the financial support provided by the Road Research Unit, National Roads Board, New Zealand, for many of the projects described here. The work of many students involved in these projects is gratefully acknowledged.

APPENDIX I. REFERENCES

Ahmad, M. (1953). "Experiments on design and behaviour of spur dikes." *Proc., Int. Hydr. Convention*, Univ. of Minnesota, Minneapolis, Minn., 145–159.
Baker, R. E. (1986). "Local scour at bridge piers in non-uniform sediment." *Rep. No. 402*, School of Engrg., The Univ. of Auckland, New Zealand.
Basak, V. (1975). "Scour at square piles." *Rep. No. 583*, Devlet Su isteri genel mudurlugu, Ankara, Turkey.
Bonasoundas, M. (1973). "Strömungsvorgang und kolkproblem." *Rep. No. 28*, Oskar v. Miller Institu, Tech. Univ., Munich, Germany (in German).
Breusers, H. N. C., Nicollet, G., and Shen, H. W. (1977). "Local scour around cylindrical piers." *J. Hydr. Res.*, 15(3), 211–252.
Chabert, J., and Engeldinger, P. (1956). "Etude des affouillements autour des piles des ponts." Laboratoire d'Hydraulique, Chatou, France (in French).
Chee, R. K. W. (1982). "Live-bed scour at bridge piers." *Rep. No. 290*, School of Engrg., The Univ. of Auckland, New Zealand.
Chiew, Y. M. (1984). "Local scour at bridge piers." *Rep. No. 355*, School of Engrg., The Univ. of Auckland, New Zealand.
Chin, C. O. (1985). "Stream bed armouring." *Rep. No. 403*, School of Engrg., The Univ. of Auckland, New Zealand.

Dongol, D. M. S. (1994). "Local scour at bridge abutments." *Rep. No. 544*, School of Engrg., The Univ. of Auckland, New Zealand.
Ettema, R. E. (1980). "Scour at bridge piers." *Rep. No. 236*, School of Engrg., The Univ. of Auckland, New Zealand.
Garde, R. J., Subramanka, K., and Nambudripad, K. D. (1961). "Study of scour around spur-dikes." *J. Hydr. Div.*, ASCE, 87(6), 23–37.
Gill, M. A. (1972). "Erosion of sand beds around spur dikes." *J. Hydr. Div.*, ASCE, 98(9), 1587–1602.
Haneu, S. (1971). "Sur le calcul des affouillements locaux dams la zone des piles des ponts." *Proc., 14th IAHR Congr.*, Int. Assn. for Hydr. Res. (IAHR), Paris, France, Vol. 3, 299–313.
Hannah, C. R. (1978). "Scour at pile groups." *Res. Rep. No. 28-3*, Civ. Engrg. Dept., Univ. of Canterbury, Christchurch, New Zealand.
Hjorth, P. (1972). "Lokal erosion och erosionsverken vid arloppsledning i kustnära områden." *Bull. Ser. B, No. 21*, Inst. for Vattenbyggnad, Tekniska Högskolan i Lund, Sweden.
Jain, S. C., and Fischer, E. E. (1979). "Scour around bridge piers at high Froude numbers." *Rep. No. FH-WA-RD-79-104*, Fed. Hwy. Admin., Washington, D.C.
Kandasamy, J. K. (1985). "Local scour at skewed abutments." *Rep. No. 375*, School of Engrg., The Univ. of Auckland, New Zealand.
Kandasamy, J. K. (1989). "Aubtment scour." *Rep. No. 458*, School of Engrg., The Univ. of Auckland, New Zealand.
Kwan, T. F. (1984). "Study of abutment scour." *Rep. No. 328*, School of Engrg., The Univ. of Auckland, New Zealand.
Kwan, T. F. (1988). "A study of abutment scour." *Rep. No. 451*, School of Engrg., The Univ. of Auckland, New Zealand.
Kwan, T. F., and Melville, B. W. (1994). "Local scour and flow measurements at bridge piers." *J. Hydr. Res.*, 32(5), 661–674.
Larras, J. (1963). "Profondeurs maximales d'erosion des fonds mobiles autour des piles en riviere." *Ann. Ponts et Chaussees*, Paris, France, 133(4), 411–424.
Laursen, E. M. (1958). "Scour at bridge crossings." *Bull. No. 8*, Iowa Hwy. Res. Board, Ames, Iowa.
Laursen, E. M. (1962). "Scour at bridge crossings." *Trans. ASCE*, 127(Part 1), 116–179.
Laursen, E. M. (1963). "Analysis of relief bridge scour." *J. Hydr. Div.*, ASCE, 89(3), 93–118.
Laursen, E. M., and Toch, A. (1956). "Scour around bridge piers and abutments." *Bull. No. 4*, Iowa Hwy. Res. Board, Ames, Iowa.
Lemos, F. O. (1975). "General report." *Proc., 16th Congr.*, Int. Assn. for Hydr. Res. (IAHR), Sao Paulo, Brazil.
Maza Alvarez, J. A. (1968). "Socovacion en cauces naturales." *Rep. No. 114*, A. J. Miguel-Rodriguez, translator, School of Engrg., Univ. of Auckland, New Zealand.
Melville, B. W. (1975). "Local scour at bridge sites." *Rep. No. 117*, School of Engrg., The Univ. of Auckland, New Zealand.
Melville, B. W. (1992). "Local scour at bridge abutments." *J. Hydr. Engrg.*, ASCE, 118(4), 615–630.
Melville, B. W. (1995). "Bridge abutment scour in compound channels." *J. Hydr. Engrg.*, ASCE, 121(12), 863–868.
Melville, B. W., and Ettema, R. (1993). "Bridge abutment scour in compound channels." *Proc., Hydr. Engrg. '93*, ASCE, New York, N.Y., 767–772.
Melville, B. W., and Dongol, D. M. S. (1992). "Bridge scour with debris accumulation." *J. Hydr. Engrg.*, ASCE, 118(9), 1306–1310.
Melville, B. W., and Raudkivi, A. J. (1977). "Flow characteristics in local scour at bridge piers." *J. Hydr. Res.*, 15, 373–380.
Melville, B. W., and Raudkivi, A. J. (1994). "Effects of foundation geometry on bridge pier scour." *J. Hydr. Engrg.*, ASCE, 122(4), 203–209.
Melville, B. W., and Sutherland, A. J. (1988). "Design method for local scour at bridge piers." *J. Hydr. Engrg.*, ASCE, 114(10), 1210–1226.
Parola, A. C., Fenske, T. C., and Hagerty, D. J. (1994). "Damage to highway infrastructure 1993 Mississippi River basin flooding." *Proc., Hydr. Engrg., '94*, ASCE, New York, N.Y., 26–30.
Raudkivi, A. J. (1986). "Functional trends of scour at bridge piers." *J. Hydr. Engrg.*, ASCE, 112(1), 1–13.
Raudkivi, A. J., and Ettema, R. (1977). "Effect of sediment gradation on clear-water scour." *J. Hydr. Div.*, ASCE, 103(10), 1209–1212.
Raudkivi, A. J., and Sutherland, A. J. (1981). "Scour at bridge crossings." *Rep. No. 51*, Rd. Res. Unit, Nat. Roads Board, Wellington, New Zealand.
Richardson, E. V., Harrison, L. J., Richardson, J. R., and Davis, S. R. (1993). "Evaluating scour at bridges." *Hydr. Engrg. Circular No. 18 (HEC-18)*, Fed. Hwy. Admin., U.S. Dept. of Transp., Washington, D.C.
Sastry, C. L. N. (1962). "Effect of spur-dike inclination on scour characteristics," ME thesis, Univ. of Roorkee, India.
Shen, H. W., Schneider, V. R., and Karaki, S. S. (1966). "Mechanics of local scour." *Rep.*, U.S. Dept. of Commerce, Nat. Bureau of Standards, Inst. for Appl. Technol., Washington, D.C.
Sturm, T. W., and Janjua, N. S. (1994). "Clear-water scour around abutments in floodplains." *J. Hydr. Engrg.*, ASCE, 120(8), 956–972.
Zaghloul, N. A. (1983). "Local scour around spur dikes." *J. Hydro.*, Amsterdam, The Netherlands, 123–140.

APPENDIX II. NOTATION

The following symbols are used in this paper:

A = area of flow obstructed by an abutment and approach fills;
b = width of a pier;
D = diameter of a circular cylindrical pier;
D_d = diameter of a debris raft;
D_e = diameter of a uniform pier that is equivalent to a nonuniform pier or a pier with a debris raft;
D_p = pile diameter;
D^* = foundation diameter of a nonuniform pier;
d_{max} = maximum particle size for a nonuniform sediment;
d_s = equilibrium depth of scour below mean bed level;
d_{50} = median particle size;
d_{50a} = median particle size of the coarsest armor layer;
K_d = particle size factor;
K_G = channel geometry factor;
K_I = flow intensity factor;
K_s = foundation shape factor;
K_s^* = adjusted foundation shape factor;
K_{yw} = flow depth-foundation size expression (m);
K_{yb} = flow depth-pier size expression (m);
K_{yL} = flow depth-abutment length expression (m);
K_θ = foundation alignment factor;
K_θ^* = adjusted foundation alignment factor;
L = projected abutment length including bridge approach (measured perpendicular to the flow);
L^* = width of the flood channel of a compound channel;
l = pier length;
n = Manning roughness coefficient for the main channel;
n^* = Manning roughness coefficient for the flood channel;
S_p = center-to-center spacing of piles in a pile group;
T_d = thickness of a debris raft;
u_c^* = critical shear velocity defined by Shields' function for d_{50} size;
u_{ca}^* = critical shear velocity of an armored bed;
V = mean approach flow velocity;
V_a = mean approach flow velocity at the armor peak = $0.8V_{ca}$;
V_c = mean approach velocity at the threshold condition;
V_{ca} = maximum mean flow velocity for armoring of the channel bed to occur;
V^* = mean approach flow velocity in the flood channel;
V_c^* = mean approach velocity in the flood channel at the threshold condition;
W = transverse dimension of pier or abutment, $\equiv b$ for piers, $\equiv L$ for abutments;
y = approach flow depth;
y^* = approach flow depth in the flood channel;
Z = height above bed level of the foundation top of a nonuniform pier;
θ = angle of bridge foundation with respect to the approach flow; and
σ_g = geometric standard deviation of the particle size distribution.